AGATA Detector Library

Second AGATA-GRETINA tracking arrays collaboration meeting

R. Hirsch, B. Birkenbach, B. Bruyneel, L. Lewandowski, P. Reiter
IKP, Universität zu Köln

04.04.2018

Components of γ-ray tracking

1

Highly segmented HPGe detectors

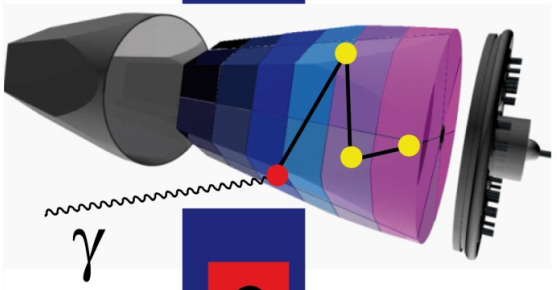

2

Digital electronics to record and process segment signals

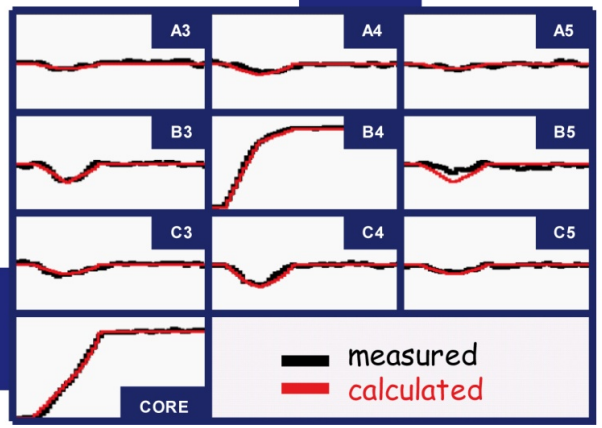

3

Identified interactions i

(x,y,z,E,t)

Pulse Shape Analysis to decompose recorded waves

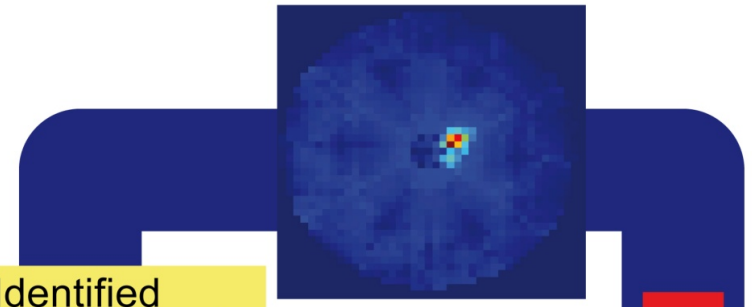

4

Reconstruction of tracks e.g. by evaluation of permutations of interaction points

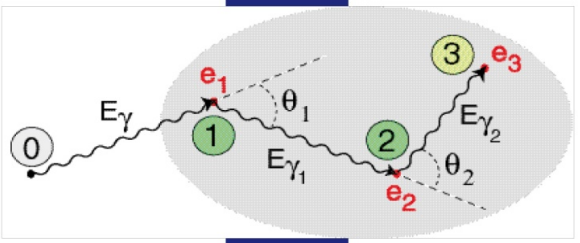

reconstructed γ-rays

Pulse-shape analysis

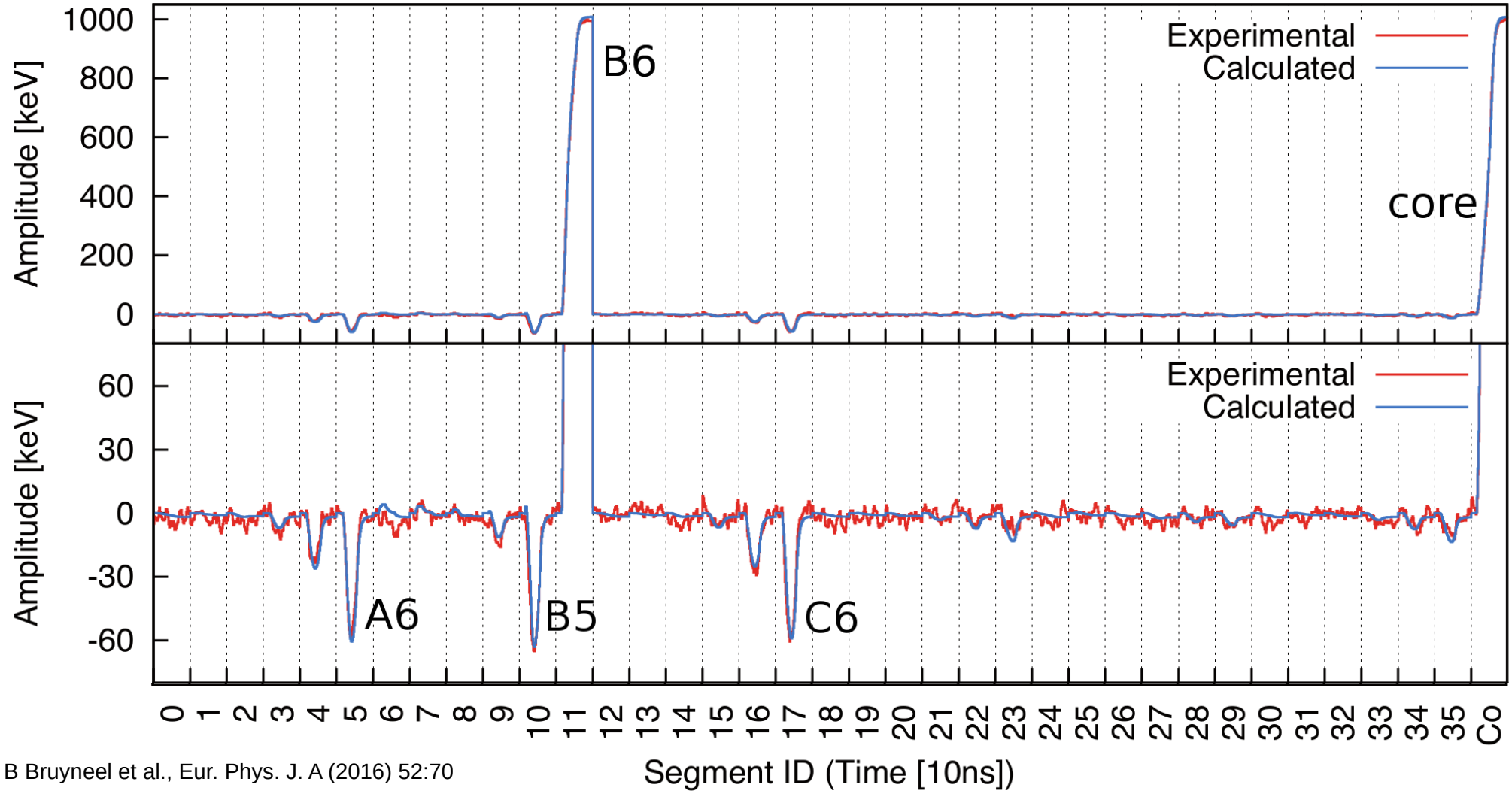

B Bruyneel et al., Eur. Phys. J. A (2016) 52:70

Database of signals with known interaction position

- Grid of interaction points
- Comparison of measured and data base signals
- Simulated database with ADL

The AGATA Detector Library

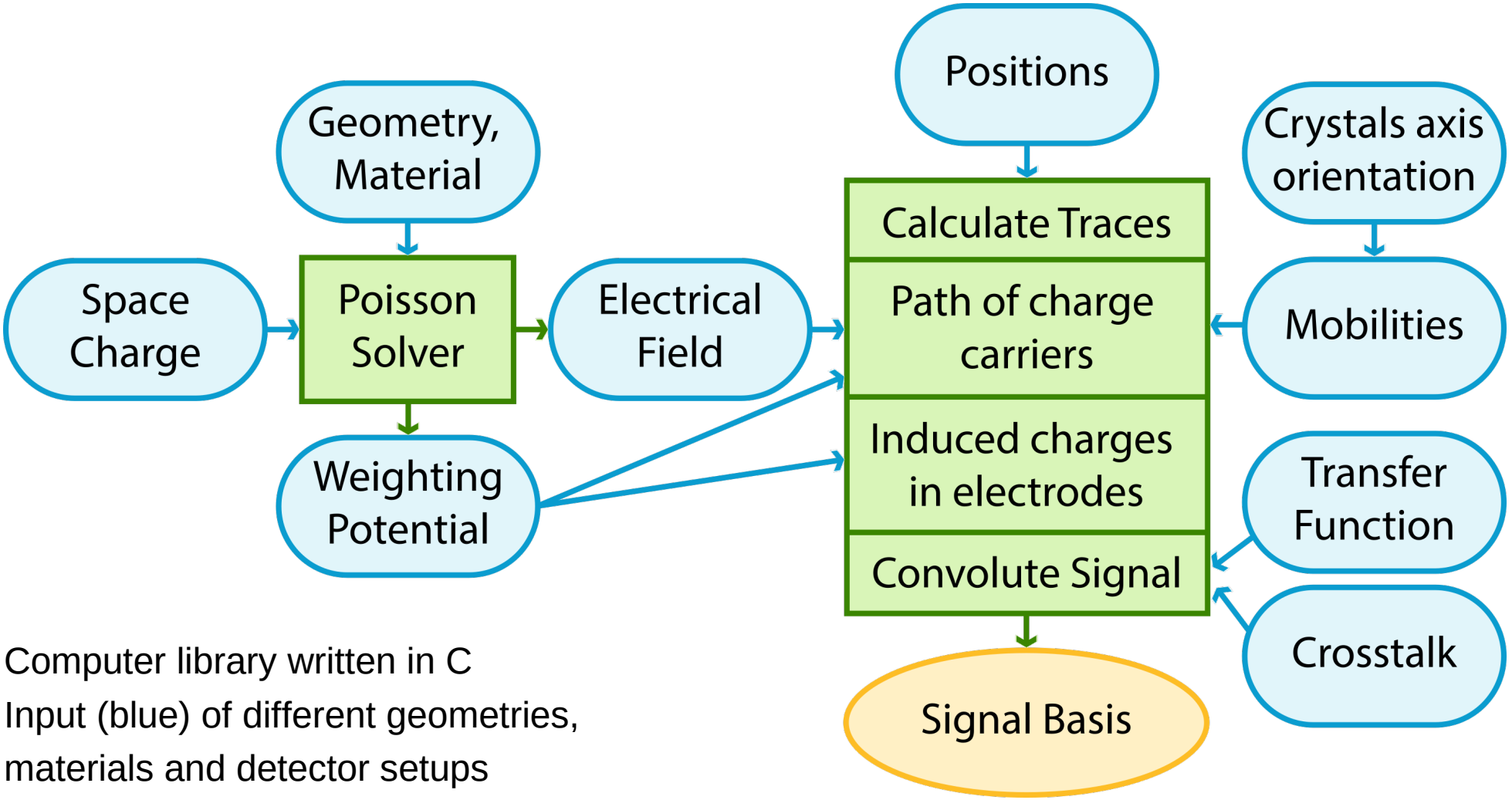

- Computer library written in C
- Input (blue) of different geometries, materials and detector setups
- Easy to extend by additional routines (green)

B. Bruyneel et al. Eur. Phys. J. A (2016) 52: 70

Signal basis

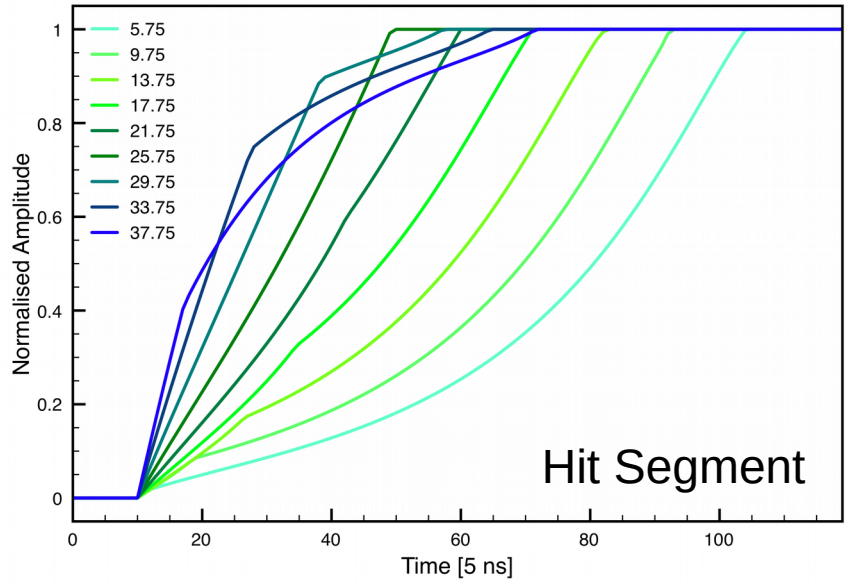

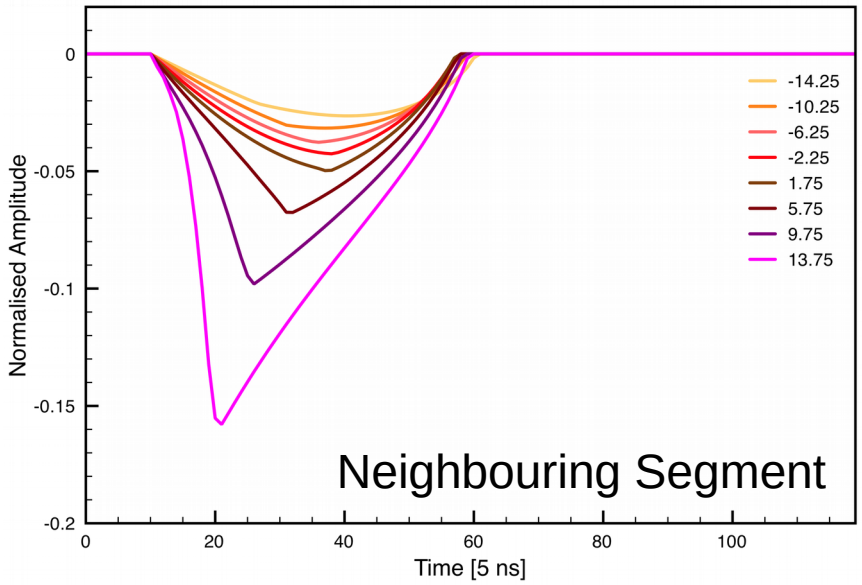

Only dependent on crystal properties:

- Shape
- Crystal axis orientation
- Impurity concentration

No signal convolution:

- Crosstalk
- Transfer function

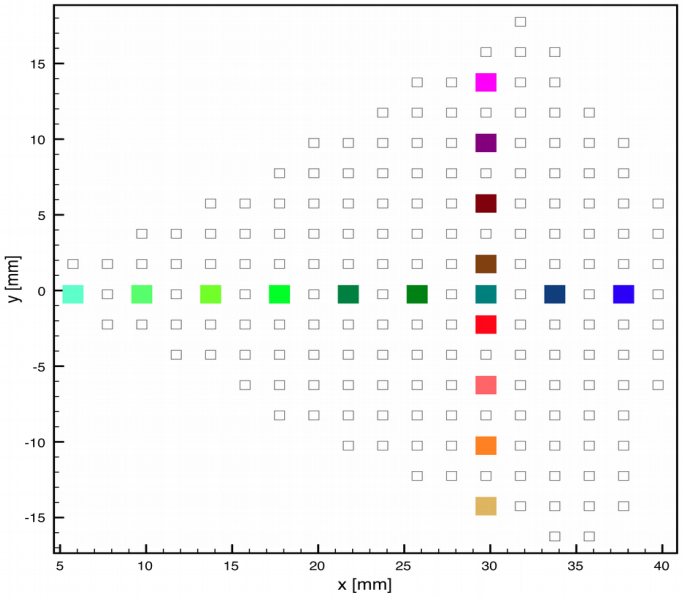

Weighting potentials

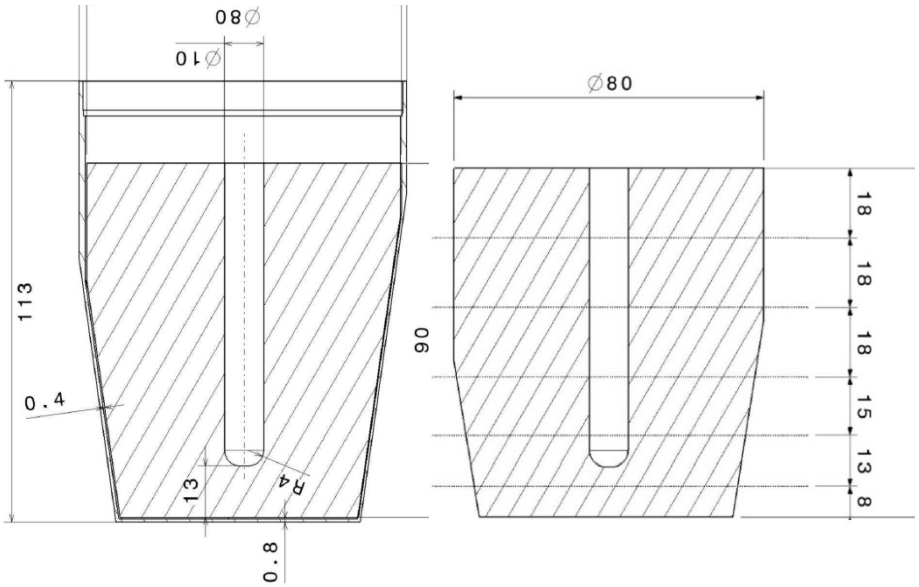

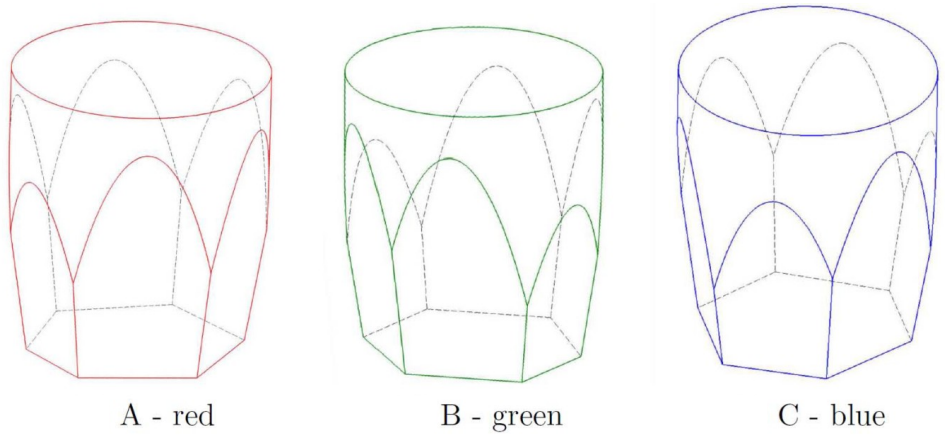

Core

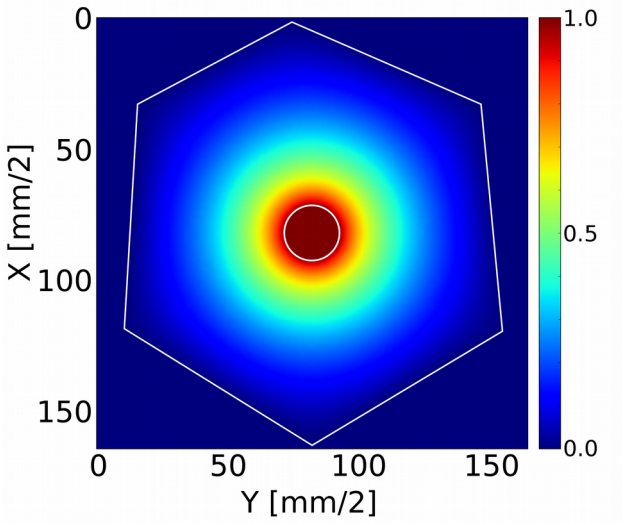

Segment

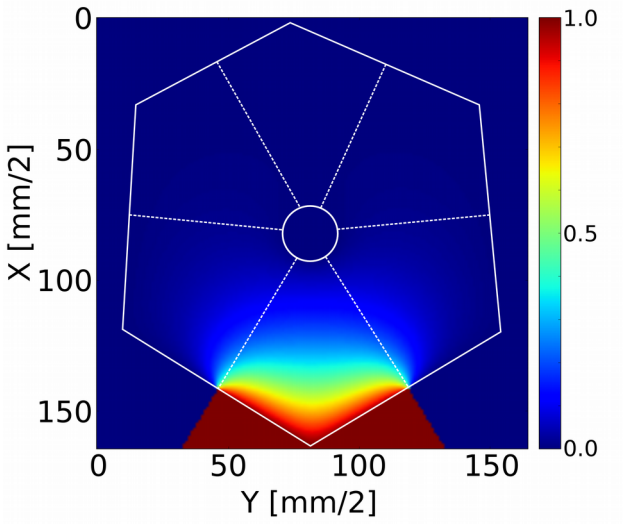

Weighting potentials

- Geometry dependent
- Cubic grid (SIMION format)
- Numerical solution
- Independent of space charge

Induced charges in electrodes

Weighting Potential
(Shockley-Ramo)

Induced charge from electrons and holes is given by:

$$Q_{qi}(t)=q[\phi_i(x_e(t))-\phi_i(x_h(t))]$$

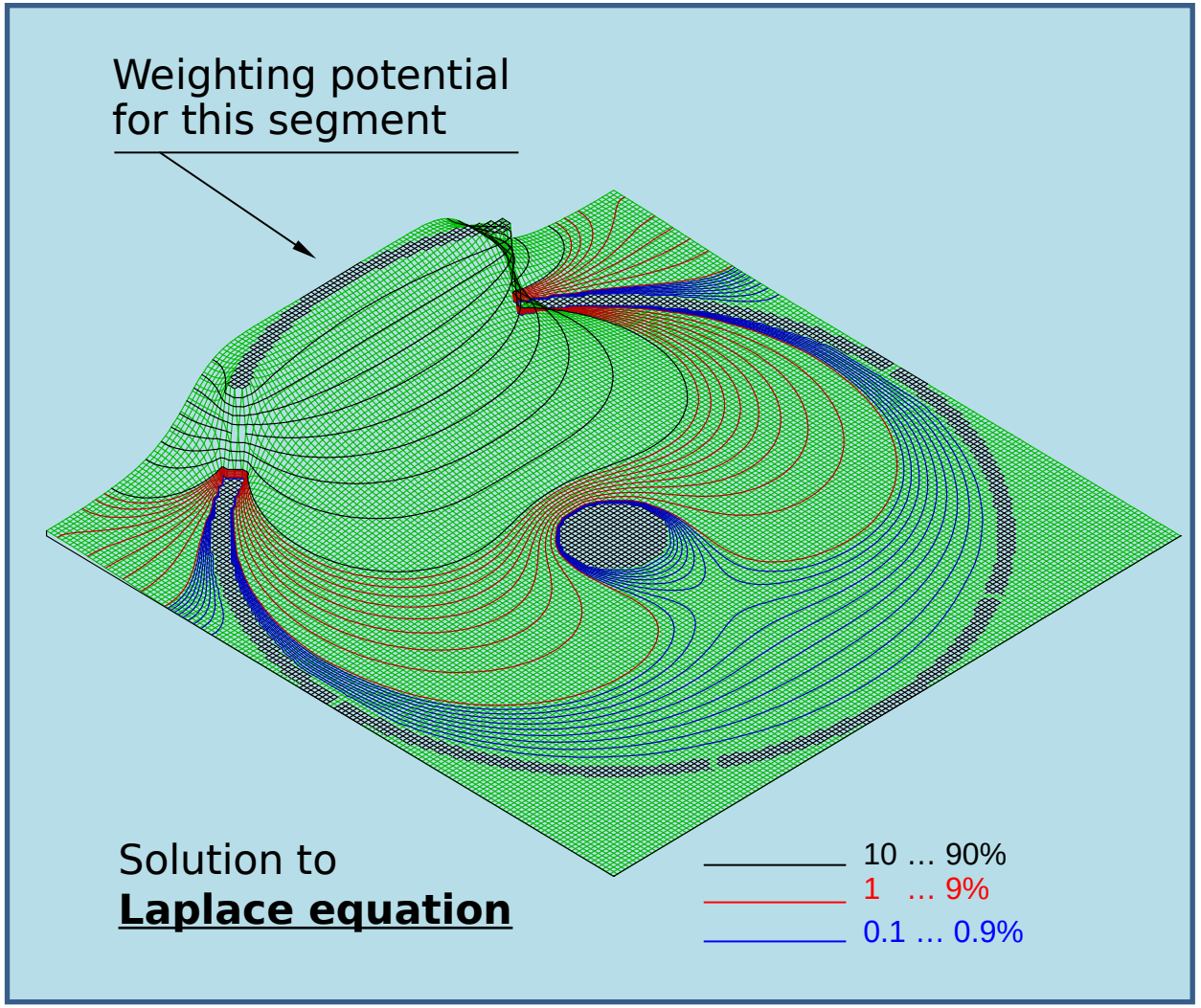

B. Bruyneel NIMA 569 (2006) 764-773

B. Bruyneel NIMA 569 (2006) 774-789

Overview

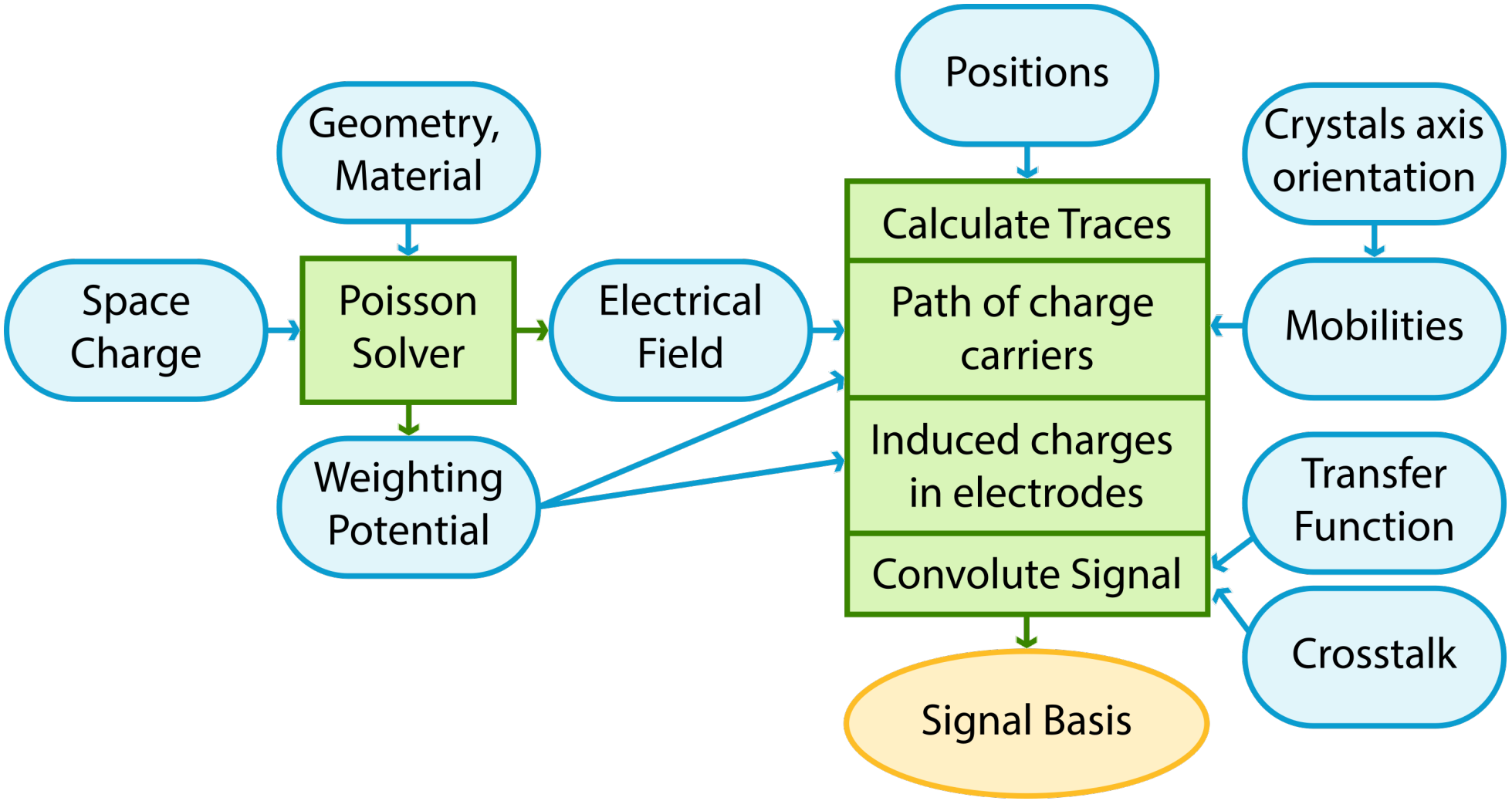
Positions
Geometry, Material
Crystals axis orientation
Calculate Traces
Space Charge
Poisson Solver
Electrical Field
Path of charge carriers
Mobilities
Induced charges in electrodes
Weighting Potential
Transfer Function
Convolute Signal
Crosstalk
Signal Basis

Space charge

Impurity concentrations

- 45 crystals
- Min. 0.35 x 10^{10} cm^{-3}
- Max. 1.97 x 10^{10} cm^{-3}

- Verified by measurements
- Radial symmetry
- Approx. linear gradient front to back

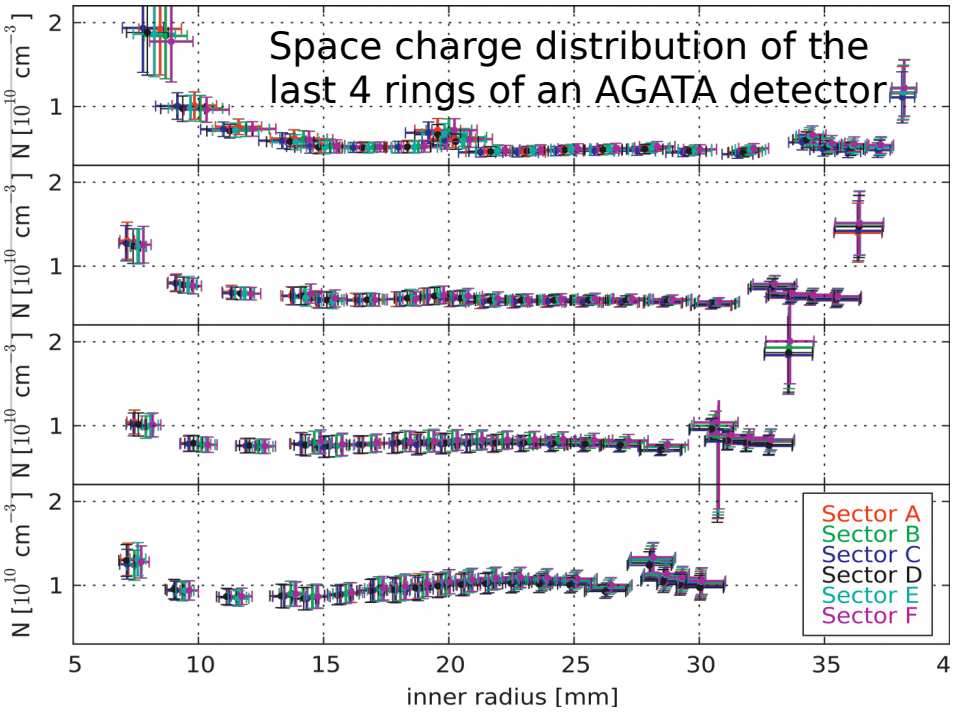

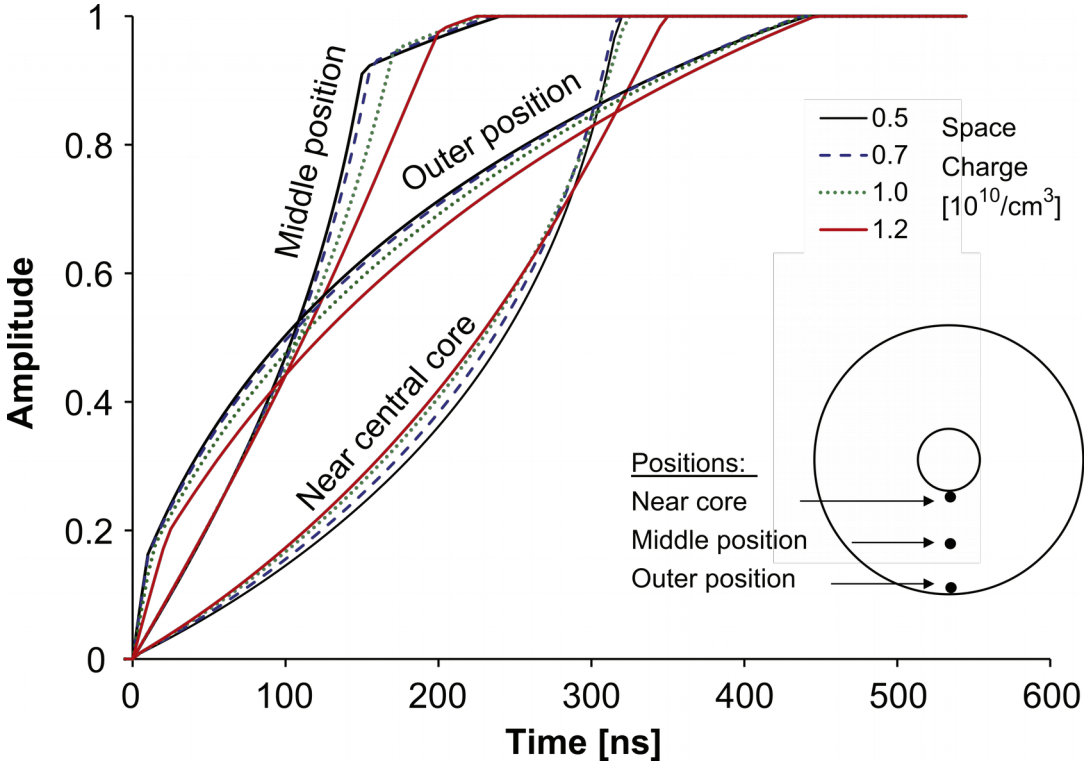

B. Bruyneel et al. NIM A 641 (2011) 92–100

B. Birkenbach et al. NIM A 640 (2011) 176–184

Charge carrier mobility

Charge carrier mobility

- Depends on:
  - Applied electrical field
  - Crystal axis orientation
- Different for electrons and holes

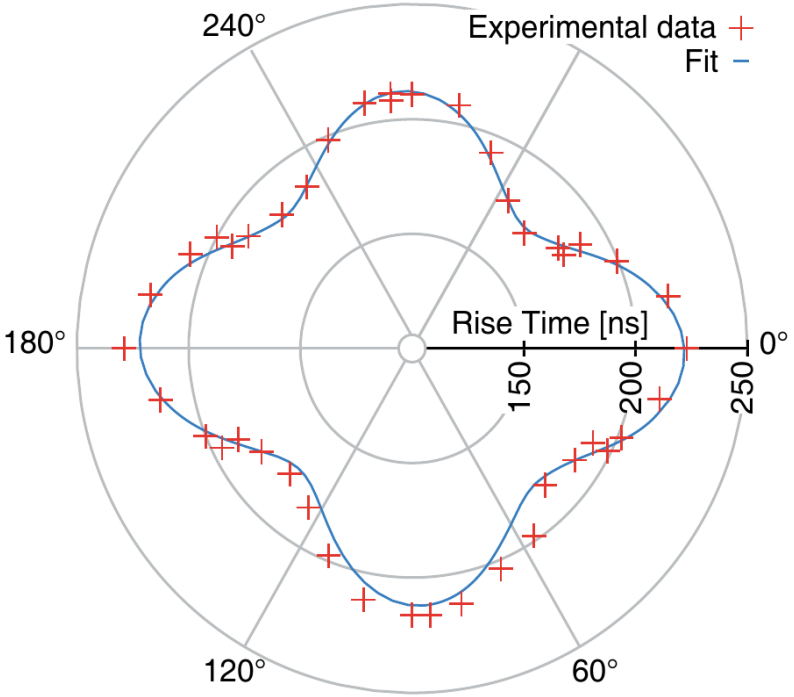

Rise time in ns for different angles

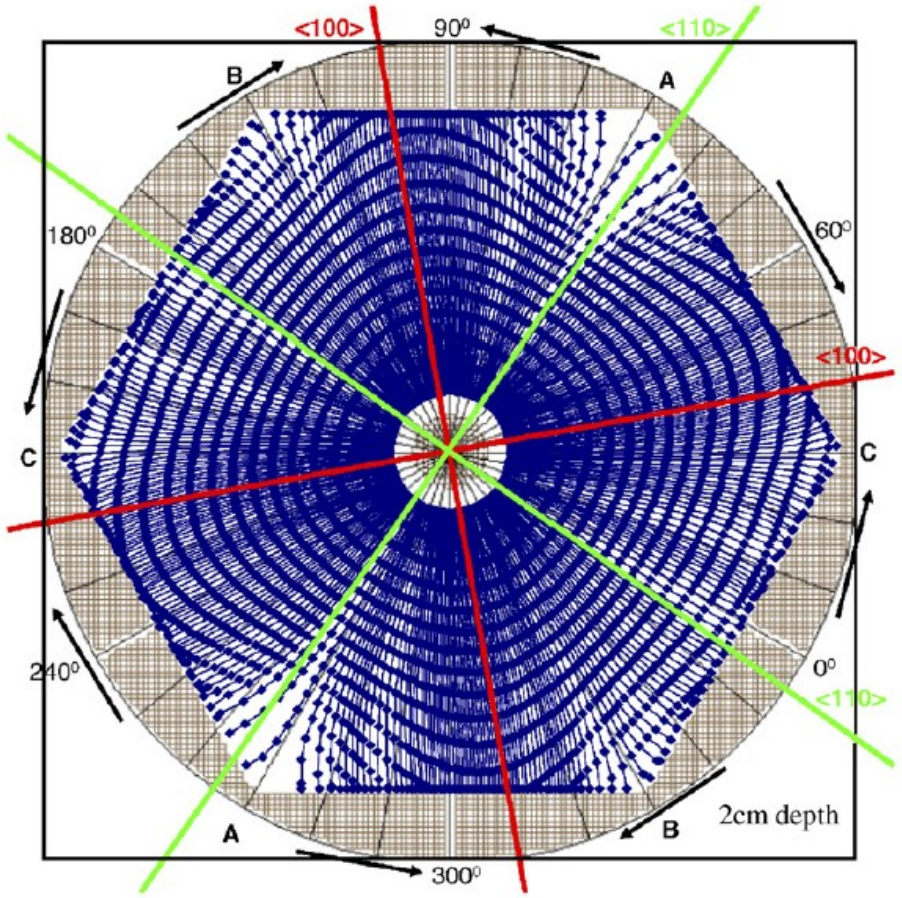

B. Bruyneel et al. Eur. Phys. J. A (2016) 52: 70

B. Bruyneel et al. NIMA 569 (2006) 774-789

Overview

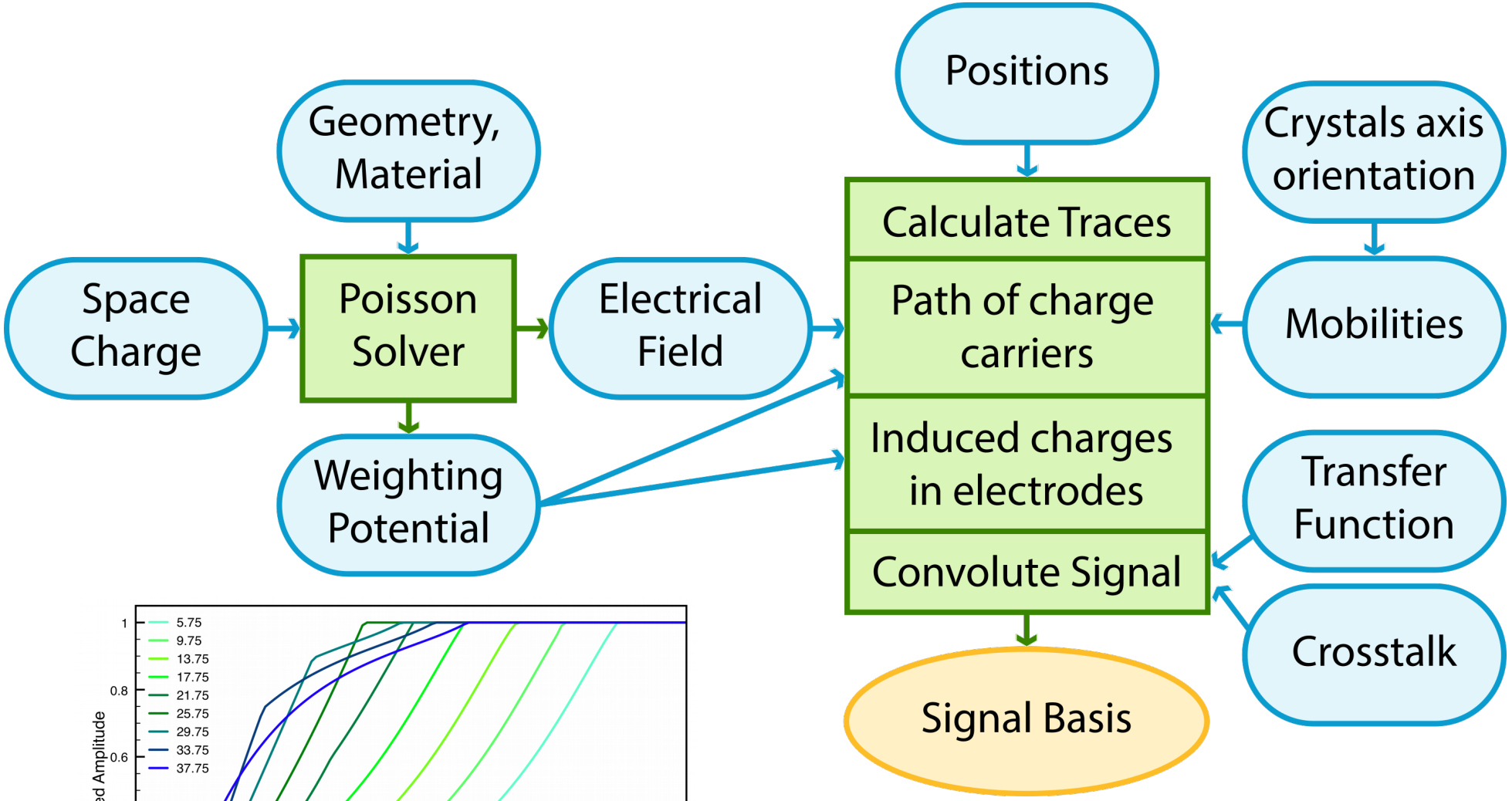
Positions
Geometry, Material
Crystals axis orientation
Calculate Traces
Space Charge
Poisson Solver
Electrical Field
Path of charge carriers
Mobilities
Weighting Potential
Induced charges in electrodes
Transfer Function
Convolute Signal
Crosstalk
Signal Basis
Normalised Amplitude
Time [5 ns]
5.75
9.75
13.75
17.75
21.75
25.75
29.75
33.75
37.75

Charge carrier trapping

Before

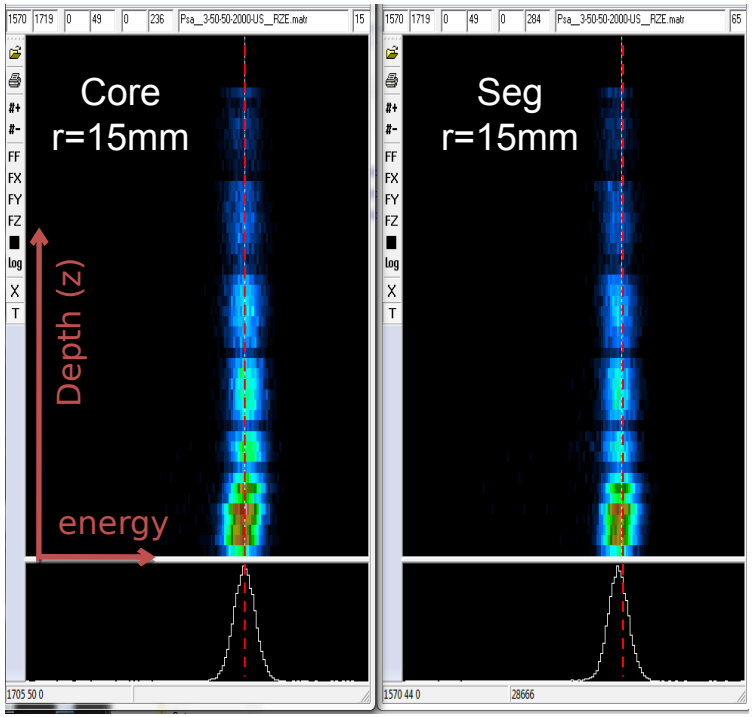

After

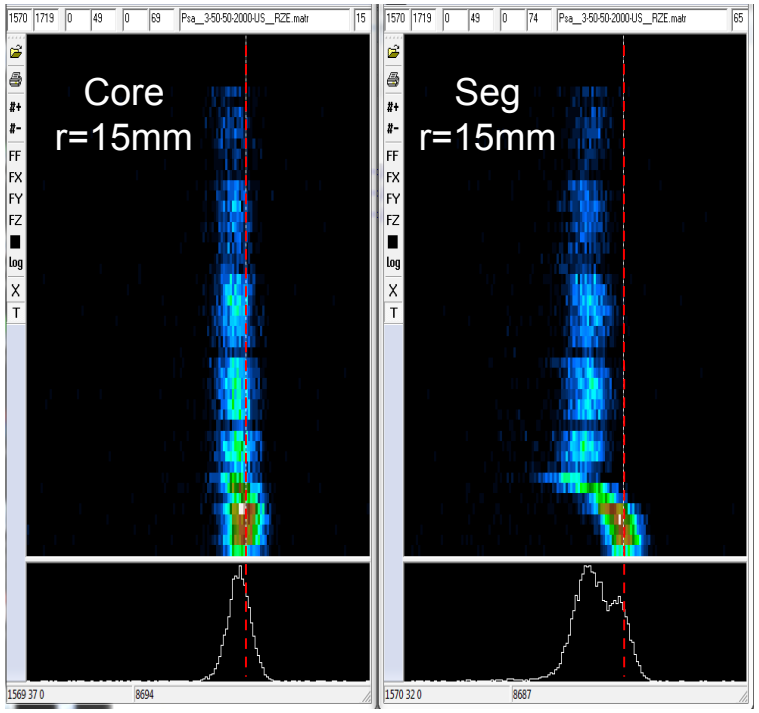

The 1332 keV peak as a function of crystal depth (z) for interactions at r = 15mm

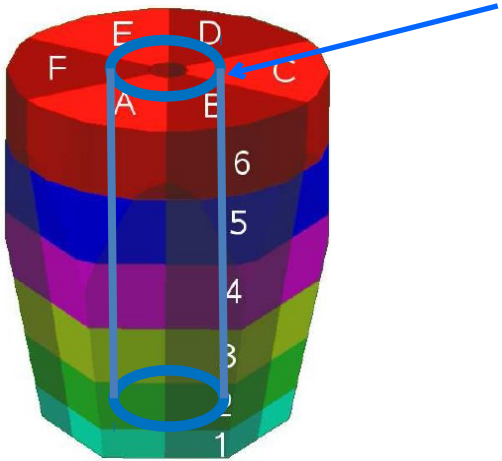

- Charge carrier loss due to neutron damage
- Proportional to the path length to the electrodes
- PSA barely affected
- Knowledge of interaction position
- Correction possible

Summary

- **Simulation input**
  - Linear space charge distributions
  - Weighting potentials
  - Anisotropic charge carrier mobility model

- **AGATA signal basis**
  - Type A,B,C
  - Impurity concentration
  - Bias Voltage
  - (Crystal axis orientation)

- **Spacial resolution**
  - 4-5 mm P.A. Söderström et al., NIM A 638, 96 (2011)

- **Results**
  - Simulated pulse shapes
  - Trapping sensitivities

Thank you for your attention!

ADL – Weighting potentials

Core electrode

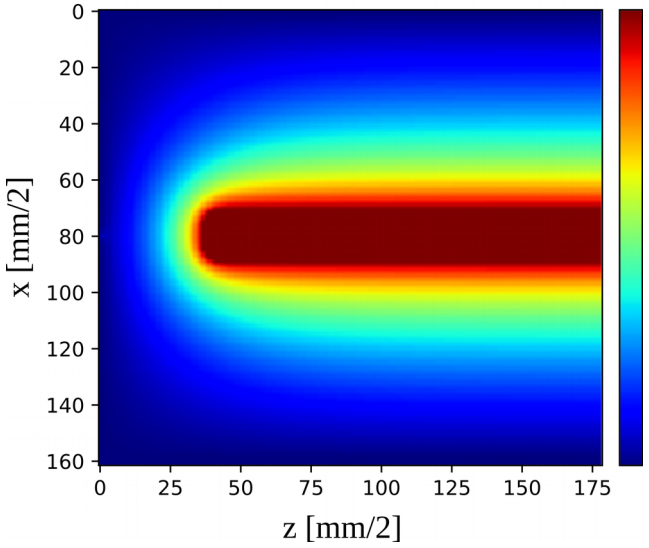

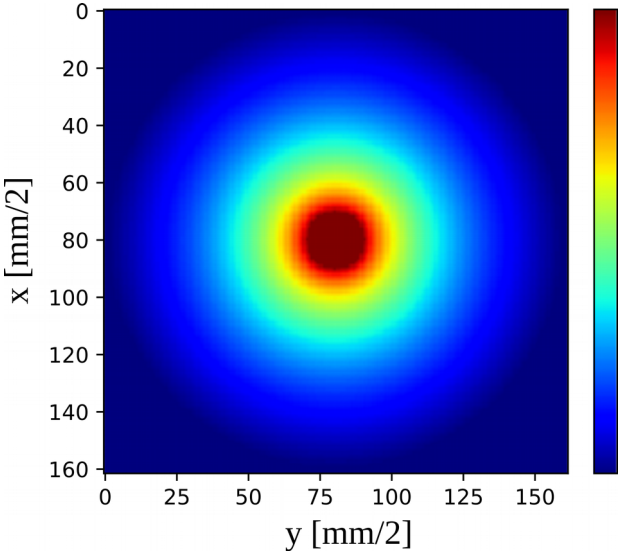

Segment C3

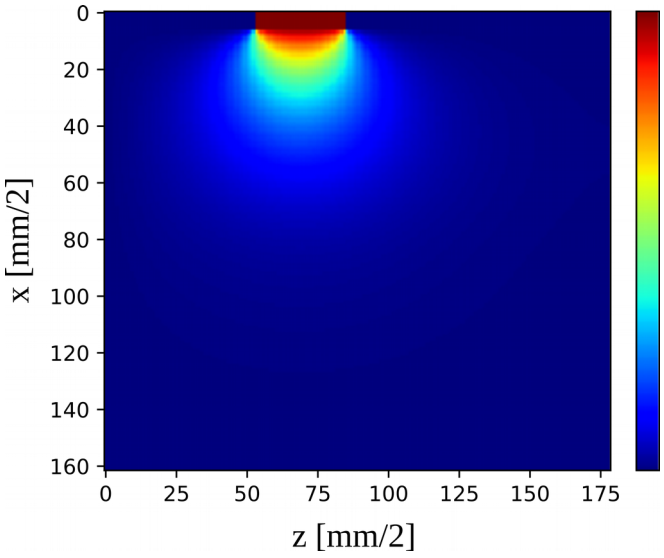

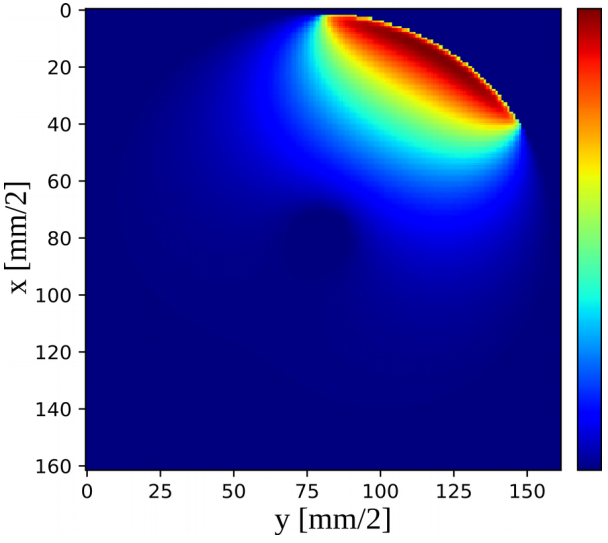

Measured Impurity Concentrations

Impurity concentration given by the manufacturer:

- front: 1.8 x 10^{10} cm^{-3}
- back: 0.5 x 10^{10} cm^{-3}

Measured height dependence

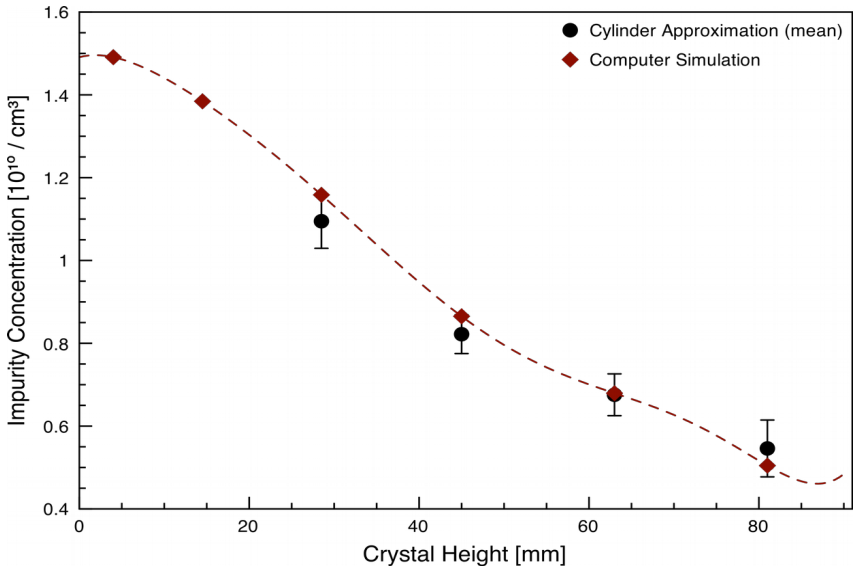

Measured radial dependence

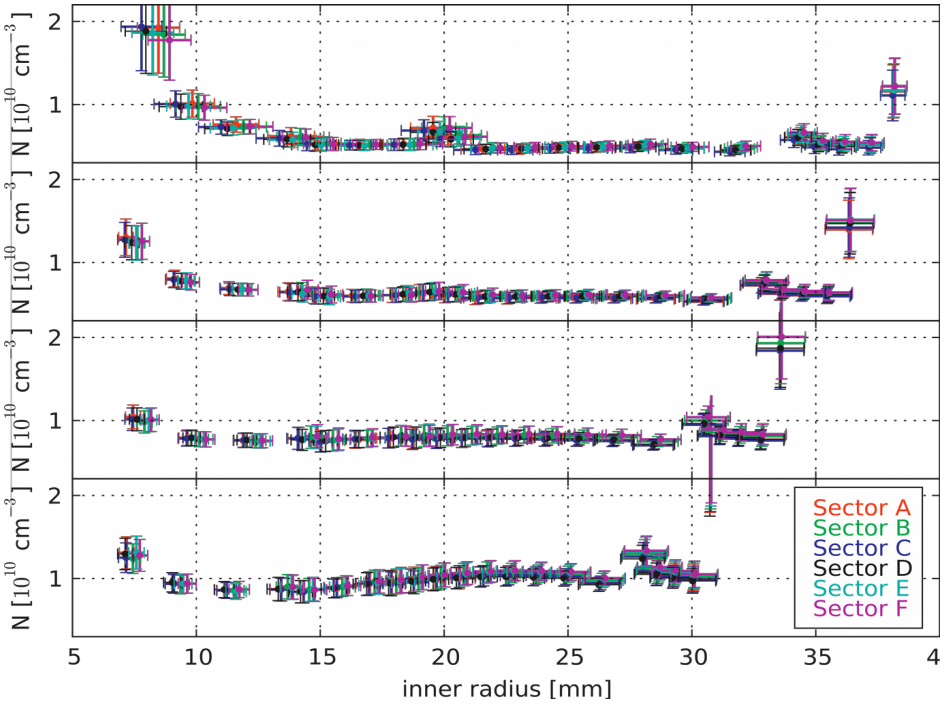

B. Birkenbach et al. NIM A 640 (2011) 176–184

Influence of crystal orientation

^{56}Fe at 220 MeV ☾ ^{197}Au, E_γ 847 keV; ^{56}Fe recoils detected in DANTE; β = 8%

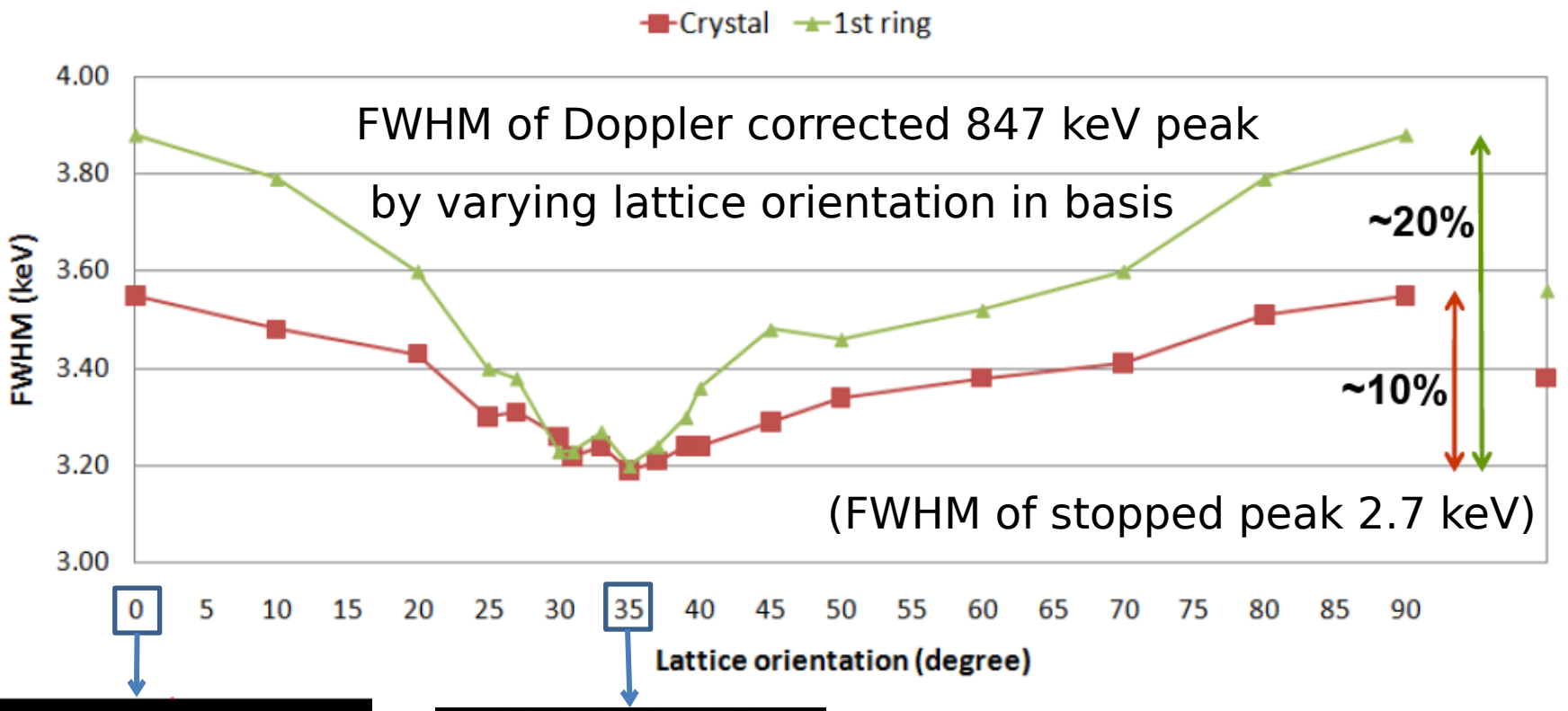

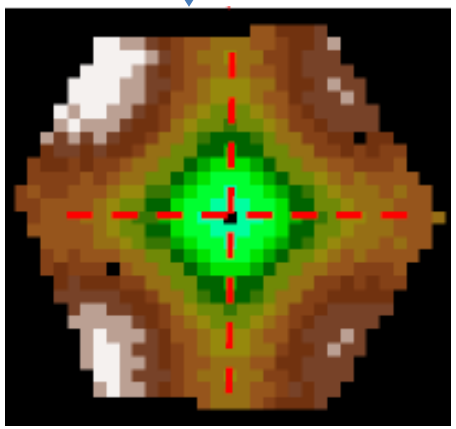

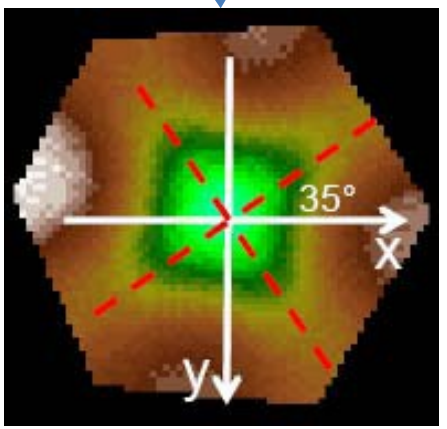

Main improvement in 1st ring
Front view of T10-90simulations
Angles with respect to x-axis

	R	G	B
ATC1	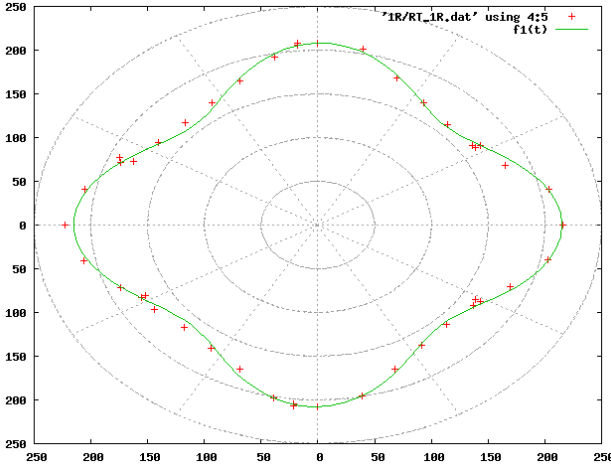	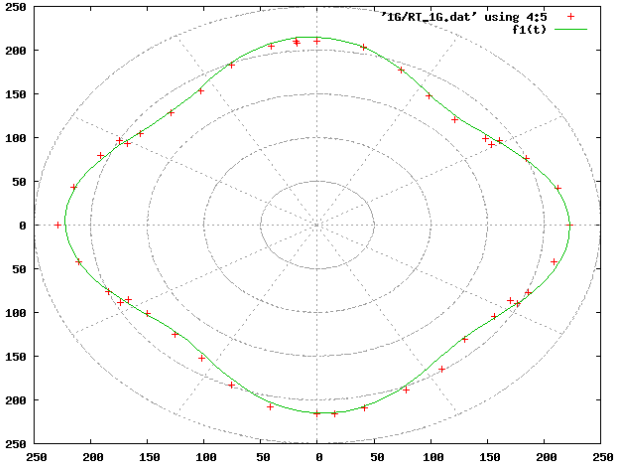	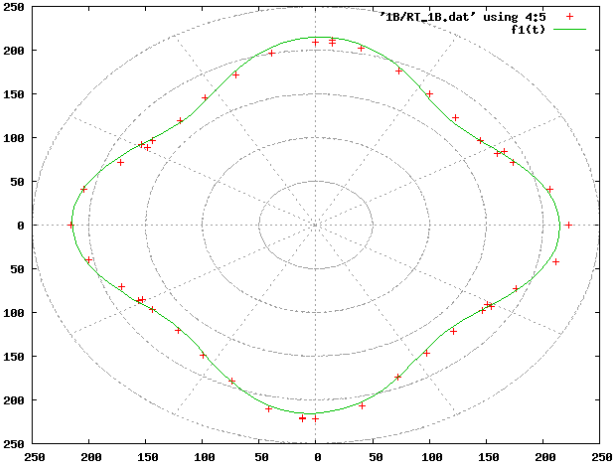
ATC2	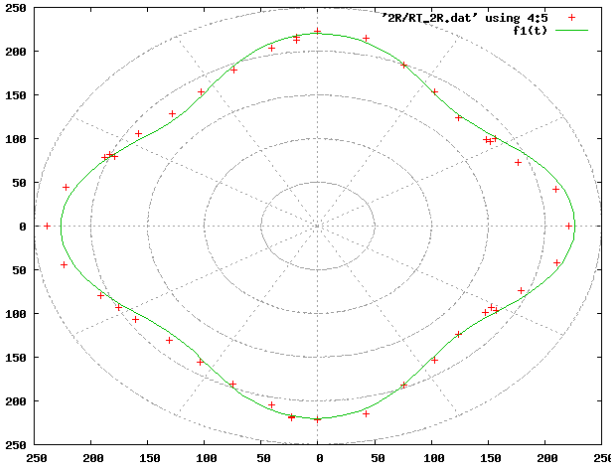	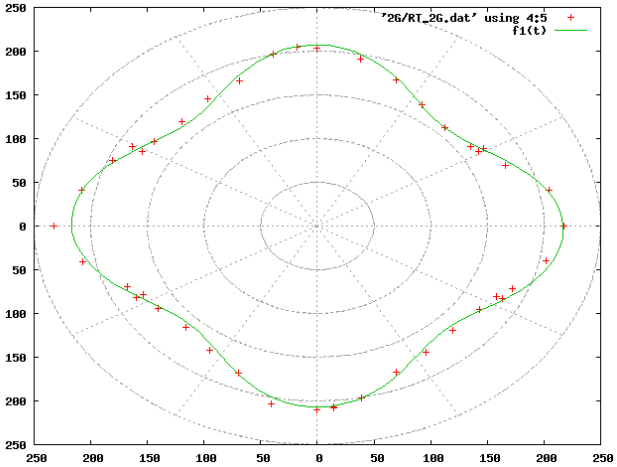	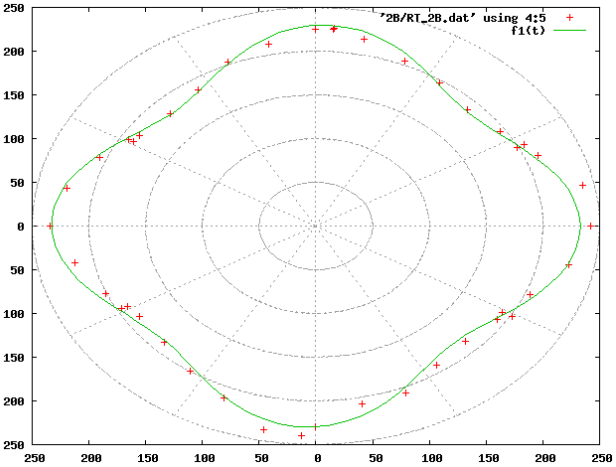
ATC4	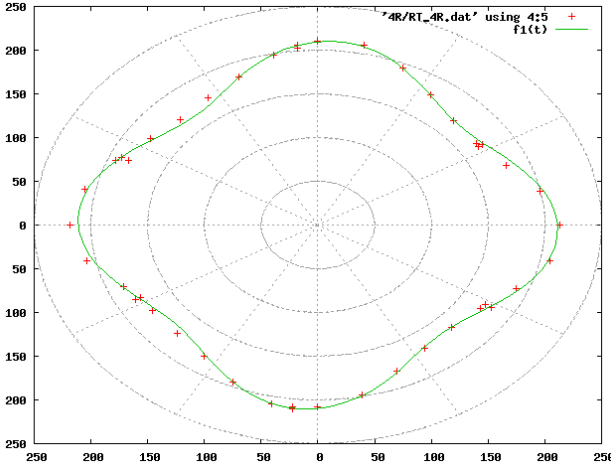	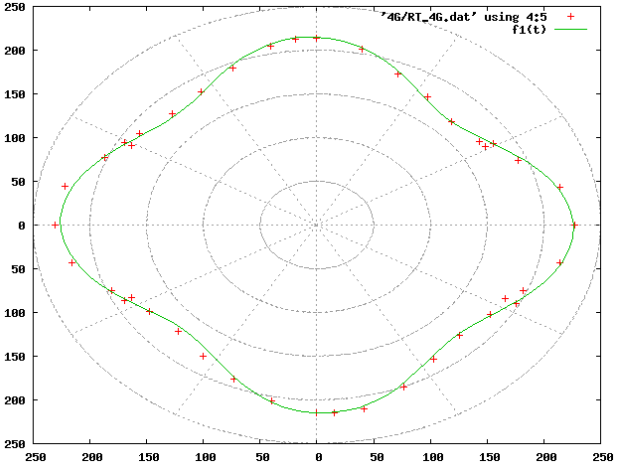	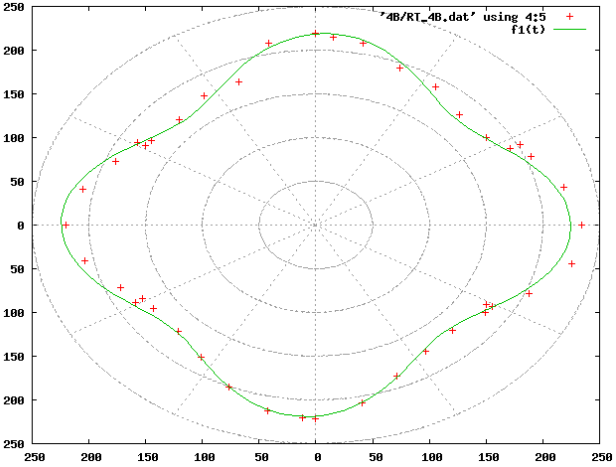

Electron mobility parameters			
Mobility along $\langle 100 \rangle$		Inter valley scattering rate	
E_0 [V/cm]	507.7	E_0 [V/cm]	1200
β	0.804	ν_0	0.459
μ_0 [cm^2/V s]	37165	ν_1	0.0294
μ_n [cm^2/V s]	-145	ν_2	0.000054

Hole mobility parameters			
Mobility along $\langle 100 \rangle$		Mobility along $\langle 111 \rangle$	
E_0 [V/cm]	181.9	E_0 [V/cm]	143.9
β	0.735	β	0.749
μ [cm^2/V s]	62934	μ [cm^2/V s]	62383

B. Bruyneel et al. Eur. Phys. J. A (2016) 52: 70

Sensitivity $s^{i}_{e,h}$

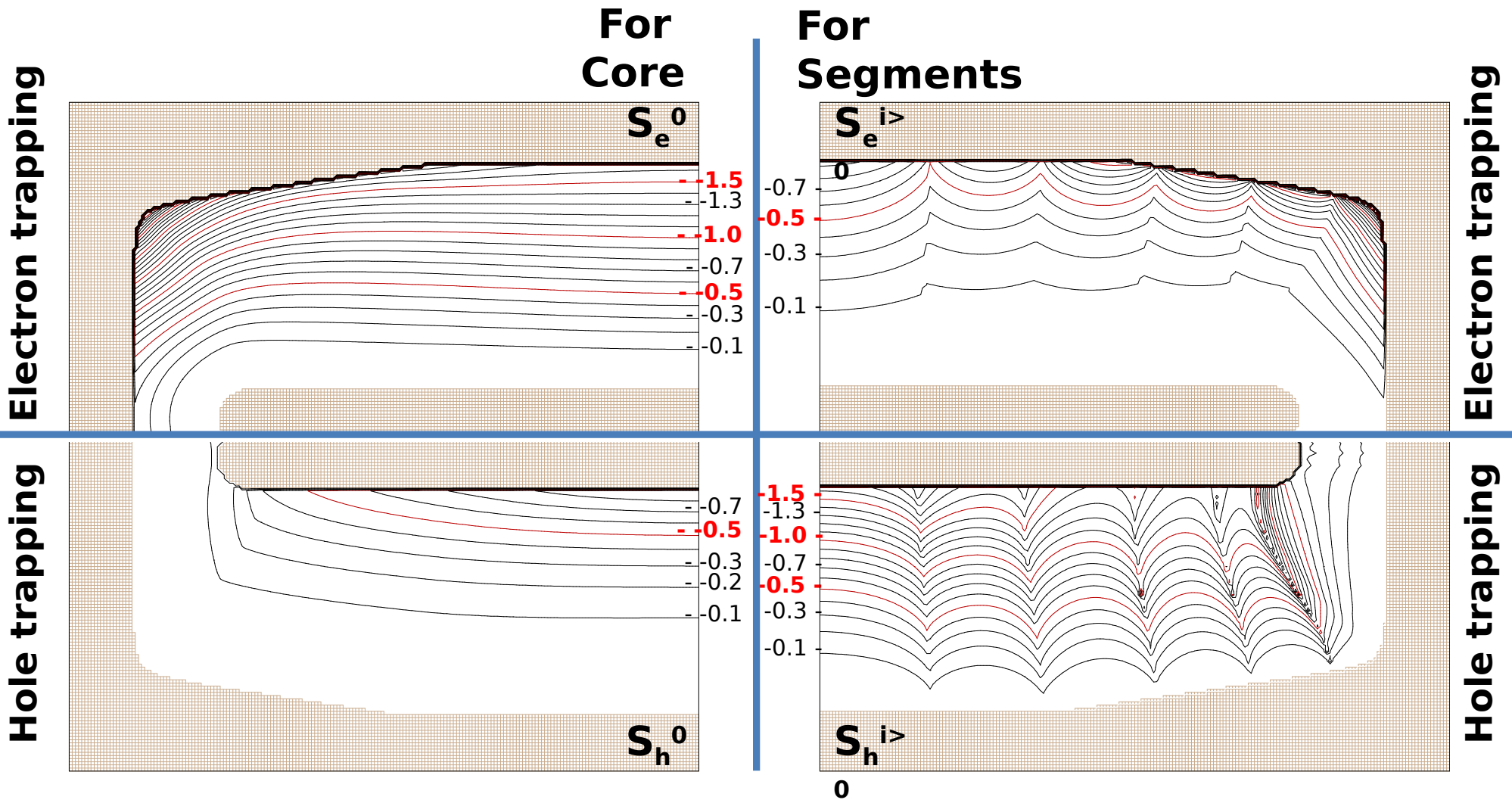

- Core more sensitive to E-trapping
- Segments more sensitive to H-trapping
- E-trapping maximal at large radius
- H-trapping minimal at large radius